Fusion Engineering and Design 18 (1991) 265–274
North-Holland

Post-analysis for the line source phase IIIA experiments of the USDOE/JAERI collaborative program on fusion neutronics

M.Z. Youssef, A. Kumar and M.A. Abdou

University of California at Los Angeles, Los Angeles, CA 90024, USA

Y. Oyama, K. Kosako and T. Nakamura

Japan Atomic Energy Research Institute, Toka-mura, Naka-gun, Ibaraki-ken, 319-11 Japan

Experimental simulation to a line source has been realized at FNS, JAERI, within the USDOE/JAERI collaborative Program on Fusion Neutronics. This simulation achieved by cyclic movement of an annular Li_2O test assembly relative to a stationary point source was a step forward in better simulation of the energy and angular distributions of the incident neutron source found in Tokamak plasmas. Thus, in comparison to other experiments previously performed with a stationary point source in the program, the uncertainties (that are system-dependent) in calculating important neutronics parameters, such as tritium production rate, will be more representative of those anticipated in a fusion reactor. The rectangular annular assembly used is 1.3 m×1.3 m and 2 m long with a square cavity of 0.42 m×0.42 m cross-section where the simulated line source is located axially at the center. There is a 1.5 cm - thick S.S. first wall followed by a 20 cm-thick Li_2O zone and a 20 cm - thick Li_2CO_3 zone. The ends of the rectangular assembly were left open. Calculations were performed for many measured items that included tritium production rate from $^6Li(T_6)$, $^7Li(T_7)$, in-system spectrum measurements, and various activation measurements [e.g. $^{58}Ni(n, 2n)$, $^{58}Ni(n, p)$, $^{93}Nb(n, 2n)$, $^{90}Zr(n, 2n)$, $^{27}Al(n, \alpha)$, $^{115}In(n, n')$, and $^{197}Au(n, \gamma)$]. These measurements were performed in three radial drawers inside the Li_2O and Li_2CO_3 zones. Flux mapping with foil activation measurements were also performed in the axial direction ($z = -100$ cm to $z = 100$ cm) at the front surface of the assembly in the cavity with the annular blanket in place and comparison was made to the bare line-source case (without annular blanket). The US has used the DOT5.1 code along with RUFF in the deterministic calculations while MCNP was used in the Monte Carlo analysis. END F/B-V data was applied in this case. The corresponding codes/data used by JAERI are DOT3.5 along with FNSUNCL, MORSE-DD, and JENDL-3 cross-section data file. In this paper, the calculated-to-measured values, C/E, for the above-mentioned measured items will be given, as obtained individually by the US and JAERI. It will be shown that even with mechanically simulating a line-source, the present methods and codes can well predict the measured items under consideration without a particular difficulty in modeling. The C/E values for T_6 and T_7 are closer to unity (10%) than those obtained in the previous point source experiments, while the reaction rates are within 10–15% of the measured values.

1. Introduction

Phase IIIA integral fusion experiment has been conducted at the Fusion Neutronics Source (FNS) facility at Japan Atomic Energy Research Institute (JAERI) within the ongoing USDOE/JAERI Collaborative Program on Fusion Neutronics. Unlike other phases of the program in which a 14 MeV point source was utilized (Phase I: open geometry [1–3], Phase II: close geometry [4–12]), a simulated line source has been utilized in Phase IIIA experiment by moving an annular blanket assembly in a periodic motion relative to a stationary 14 MeV point source and hence produce the same effect on the neutronics characteristics of the test assembly that would have been achieved by a true line source [13–15]. Another major difference between Phase IIIA experiment and other experiments performed previously in Phase I and II is that the annular assembly totally surrounds the simulated line source. This leads to a more prototypical conditions for the incident neutron source in terms of energy and angular dependence that are closer to those found in the toroidal plasmas in Tokamaks.

The simulation of the line source has been achieved at JAERI [14] through two modes of operation, namely stepwise mode and continuous mode of operation. In the former, the D–T neutrons are generated at selected number of points along the simulated line source. These

point sources are equally separated from each other and the duration of operating the D–T neutron source is equal at each point. In the latter operation mode, the annular assembly continuously moves relative to the fixed point source in a periodic movement with a speed of 6.1 mm/s. It was shown that both modes of operation produce the same neutronics effects inside the assembly [14,15]. Several measurements have been performed for tritium production rate, spectra, and several reaction rates and the calculated results were compared to the experimental values to examine the prediction accuracies obtained by various codes and data bases. Both JAERI and the US have performed independently these analyses using their own computational tools and neutron cross-section libraries to arrive at estimates for the uncertainties involved in estimating key design parameters such as tritium production rates and in-system spectra.

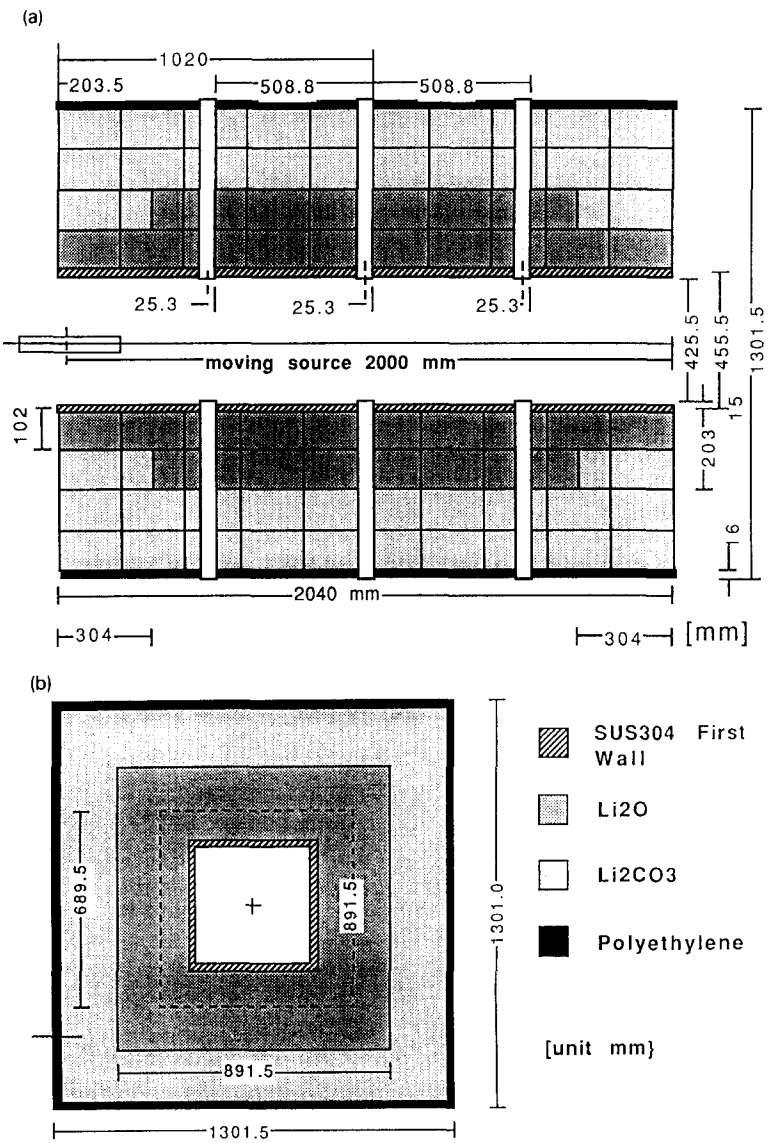

Fig. 1. Experimental arrangement for Phase IIIA experiment.

The subject of this paper is to discuss the analyses of Phase IIIA experiment as obtained by the US and JAERI. More description on the experimental techniques and results can be found in refs. [15–17]. The experiment is briefly discussed in section 2. A description of the calculational methods is given in section 3. The analytical results and the comparison with the experimental values are given in section 4. Summary of the present work is outlined in section 5.

2. The experiment

Figure 1 shows the experimental annular assembly whose length is 2040 mm and has an outer dimension of 1301 mm × 1301 mm. The inner cavity has a square shape of 425.5 mm × 425.5 mm with a 15 mm-thick 304 stainless steel first wall. The Li_2O zone is 200 mm-thick followed by a 200 mm-thick Li_2CO_3 zone whose outer surface is covered by 16 mm polyethylene (PE) layer to isolate the assembly from the room-returned neutrons. Both ends of the assembly are open to facilitate its movement relative to the long-tube water-cooled neutron target. The length of the simulated line source is 2000 mm. There are six experimental drawers in the radial direction (three on each side) that are filled with special blocks of Li_2O and Li_2CO_3 and are separated by 500 mm distance in the axial direction.

Prior to performing the in-system measurements, the simulated line source has been characterized without the annular assembly in place. This was performed by measuring several activation reactions in the axial direction ($z = -100$ cm to $z = 100$ cm) and at a distance of 219 mm from the line source. The continuous operation mode was adopted for these measurements and the multifoils (MF) were placed at eleven positions that are 200 mm apart. This also was done but with the assembly around the line source and comparisons were made to the without-the-assembly case. This was necessary to study the impact of the reflected neutrons traveling inside the inner cavity on these MFA measurements. Note that the experiments were performed in the first target room of the FNS facility which is large (~ 15 m × ~ 15 m) compared to target room no. 2 (~ 5 m × ~ 5 m) where previous experiments in Phase I through II were performed. The consequence is that the room returned neutrons component in Phase III experiments is small and does not affect the in-system measurements. For the bare source characteristics experiments, however, it is expected to find large discrepancy between calculations and measurements for non-threshold reactions such as $^{197}Au(n, \gamma)$ where reflection from the room floor (at a distance of ~ 3 m) will cause this discrepancy unless the calculational model used takes into account the floor and other equipments located near by the assembly. The reactions considered in source characterization are: $^{58}Ni(n, 2n)^{57}Ni$, $^{90}Zr(n, 2n)^{89}Zr$, $^{93}Nb(n, 2n)^{92m}Nb$, $^{27}Al(n, \alpha)^{24}Na$, $^{56}Fe(n, p)^{56m}Fe$, $^{59}Co(n, \alpha)^{56}Mn$, $^{58}Ni(n, p)^{58}Co$, $^{64}Zn(n, p)^{64}Cu$, and $^{115}In(n, n')^{115m}In$. These reactions have effective threshold energies of ~ 13 MeV, ~ 12 MeV, ~ 8 MeV, ~ 6 MeV, ~ 5 MeV, ~ 5 MeV, ~ 2 MeV, ~ 2 MeV and ~ 0.5 MeV, respectively. Also, the non-threshold reaction $^{197}Au(n, \gamma)$ was considered as an index for the thermal neutrons.

Neutron spectra above 1 MeV along the central axis of the three drawers was measured by NE2 13 detectors at four locations each. Proton recoil counter (PRC) was used to measure neutron spectrum in the energy range 1 KeV–1 MeV at the inner surface of the cavity and at a distance of 5 cm inside the Li_2O zone. Li-glass detectors were used to measure tritium production rate from $^6Li(T_6)$ inside the drawers while NE213 indirect method was used to measure tritium production rate from $^7Li(T_7)$ by folding the measured spectrum with the $^7Li(n, n'\alpha)t$ cross section. These methods are on-line and the stepwise mode of operation was adopted in this case. T_6 and T_7 were also measured inside the drawers in the continuous operation mode (long irradiation time of ~ 10 hr) by using Li_2O pellet foil technique.

3. Calculational methods

Both deterministic and Monte Carlo methods were used to analyze the experiment. The US adopted the DOT5.1 code [18] along with the RUFF [19] first collision code for the deterministic treatment while the MCNP-3B code that uses continuous energy and angle ENDF/B-V data was applied in the Monte Carlo treatment. The cross-section library used in DOT5.1 calculations (P_3-S_{16}) is the 30-group MATXS5 library [20] which is based on ENDF/B-V (version 2) data. In JAERI's analysis, the DOT3.5 code was applied in the deterministic method along with the FNSUNCL code. The latter is a modified version of GRTUNCL [21] in which multiple neutron sources and accounting for variation in their energy and angular distributions were considered. This modified version is thus equivalent to the RUFF [19] code. The FUSION-J3 library (P_5-S_{16}, 125-n, 41-g) based on JENDL-3 data was used in the DOT3.5 calculations. For the Monte Carlo calculations, the MORSE-DD [22] code was applied along with the

DDX library (125-g, double differential cross-section library based on JENDL-3).

In the 2-D calculations performed by DOT5.1 (US), the energy and angular distribution of neutrons generated at the D + beam spot on the Ti-T target was treated relativistically. It was necessary to perform first a 3-D MCNP calculations for the long tube water-cooled target in order to account for the presence of the target structure and coolant tubes and thus generate the appropriate angular/energy distributions of the incident neutrons to annular assembly. These distributions were assumed at each point source locations considered in the simulation of the line source and a single RUFF run was made to estimate the first collision neutron source needed for the DOT5.1 calculations. Notice in this approach that while neutron collisions in the target structure and coolant channels are considered in the initial MCNP run, neutrons that reach the annular assembly and reflect back to the target to interact with its structure and reflect back to the annular assembly are ignored, i.e., interactions in the annular assembly and the target structure are decoupled. This decoupling was necessary, otherwise a separate RUFF/DOT run should have been performed at each selected point source to account for the varied length of the drift tube of the target inside the cavity as one moves toward the front edge of the assembly (details of the drift tube and target structure can be found in Refs. [13–16]. Similar procedures were applied in JAERI's DOT3.5/FNSUNCL calculations. The number of equally-spaced point source locations, N, selected for the line source simulation was 26 in the US calculations and 41 in JAERI's calculations. It was shown that $N \sim 20$ is sufficient for the simulation [13]. Figure 2 shows the 2-D R-Z cylindrical model used for the deterministic methods calculations. The actual thicknesses were considered in the 2-D model although cylindrical geometry is assumed. Approximating the rectangular annular assem-

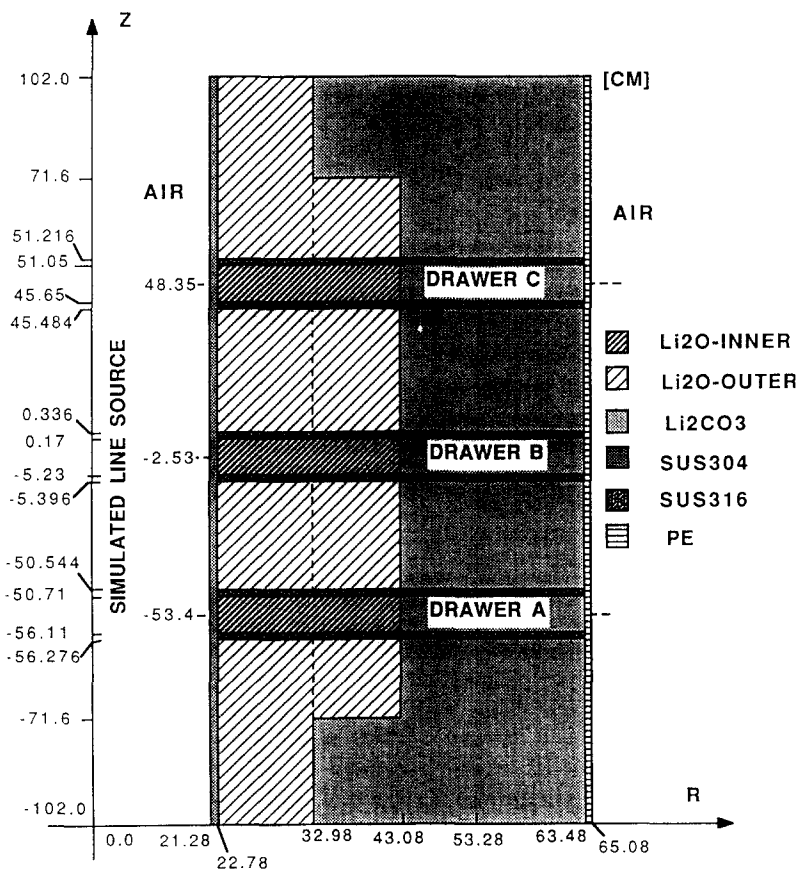

Fig. 2. The 2-D R-Z cylindrical model for DOT5.1 calculations.

bly by a cylindrical geometry is reasonable, particularly when local effects are considered.

In the Monte Carlo treatment (MCNP: US, MORSE-DD: JAERI), there is no need for the multiple point source approach followed in the DOT calculations, rather, random sampling of the energy and angular distributions of incident neutrons to the annular assembly for each position along the line source is made (continuously in MCNP calculations and from bins in the MORSE-DD calculations) from the distributions obtained from the initial Monte Carlo run for the drift tube/target calculations.

4. Calculational results and comparison to measurements

Figure 3 shows the relative intensity of neutrons emitted from the long tube water cooled target (WCT) as obtained from the initial Monte Carlo run (JAERI) for the drift tube/target alone (no assembly). Forward neutrons ($0 < \mu \leq 1$) are more than backward neutrons ($-1 \leq \mu < 0$) by ~10% due to collisions in the long drift tube. Incident neutron spectra are shown in Fig. 4 in the direction $\mu = 1$, 0, and -1 where it peaks around 15 MeV for $\mu = 1$ and at 13.6 MeV for $\mu = -1$. In the latter case, more soft neutrons are found as compared to $\mu = 1$ and $\mu = 0$ cases. Similar intensities/spectra were calculated by the US.

4.1. Source characteristics

Multifoil activation measurements were performed to characterize the simulated line source without (bare case) and with the annular assembly in place. Figure 5 shows the axial distribution in the z direction (from $z = -100$ cm to $z = 100$ cm) at a radial distance $R = 21.9$ cm from the line source for the ^{58}Ni(n, 2n) [E_{th} ~ 13 MeV), ^{27}Al(n, α) [E_{th} ~ 6 MeV] and ^{115}In(n, n')^{115m}In reactions [E_{th} ~ 0.5 MeV]. These reactions are good indices for the spectrum in the high, medium, and low energy range, respectively. As shown, the ^{58}Ni(n, 2n) reactions is larger in the front direction [$z > 0$, toward the front end] relative to the values in the

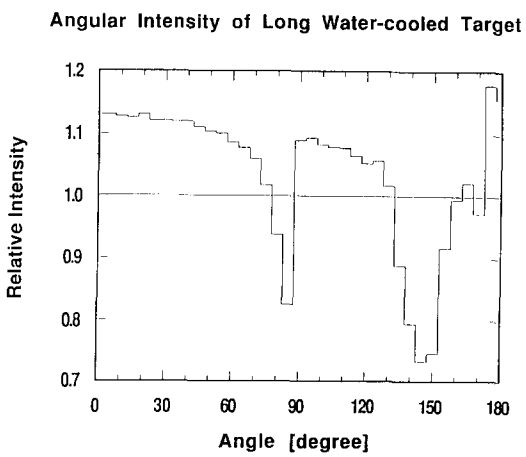

Fig. 3. Relative intensity of incident neutron source from the long tube water cooled target (JAERI's calculations).

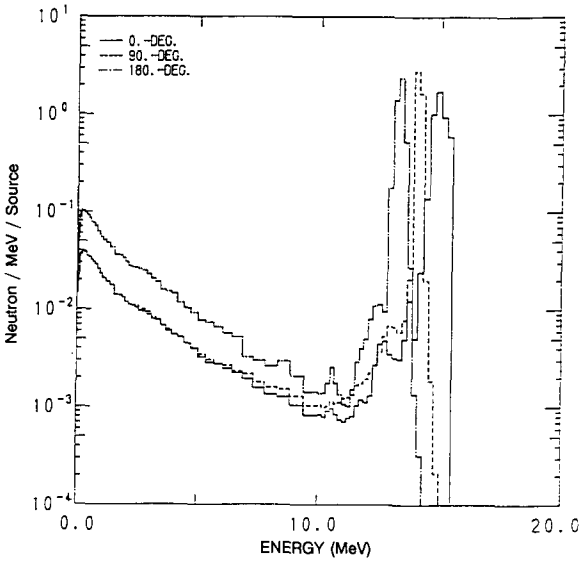

Fig. 4. Incident neutron spectrum from the long tube water cooled target (JAERI's calculations).

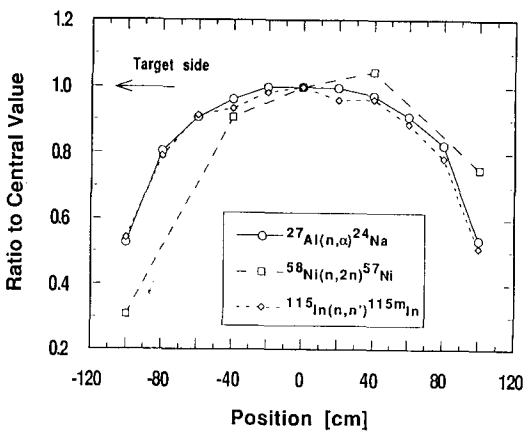

Fig. 5. Reaction rate distribution in the axial direction for ^{27}Al(n, α), ^{58}Ni(n, 2n) and ^{115}In(n, n') reactions at a radial distance $r = 21.9$ cm without the assembly (JAERI's measurements).

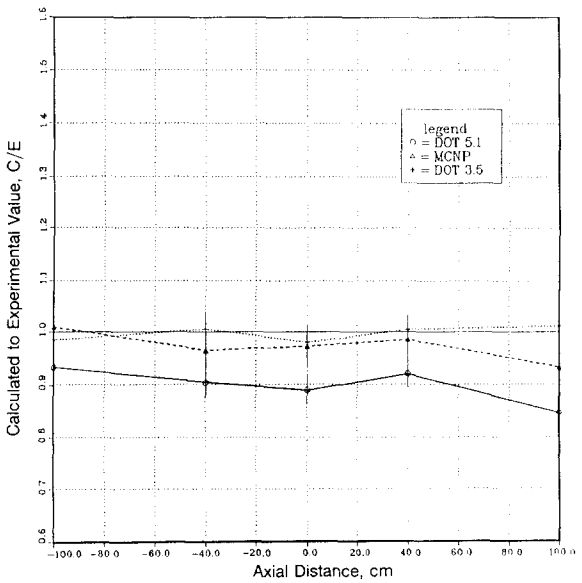

Fig. 6. C/E values for the ^{90}Zr(n, 2n)^{89}Zr reaction in the axial direction (without assembly).

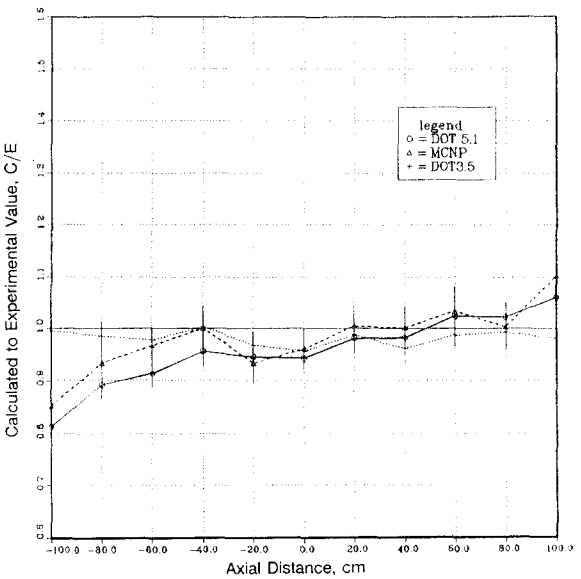

Fig. 7. C/E values for the ^{115m}In(n, n′)^{115m}In reaction in the axial direction (without assembly).

back direction [$z < 0$; toward the backend on the target side]. Locations that are toward the front end see more forward neutrons than backward neutrons as the target travels from $z = -100$ cm to $z = 100$ cm. As shown in Figs. 3 and 4, these forward neutrons are larger by ~ 10% and have also a peak around 15 MeV where the ^{58}Ni(n, 2n) cross-section is large. On the other hand, reactions such as ^{115}In(n, n′) have low threshold energies. Locations that are near the back end (target side) see more of backward neutrons than forward neutrons as the target travels inside the cavity. The backward neutrons ($\mu < 0$) are less than the forward ones (see Fig. 3), however, most of the backward neutrons have a larger low-energy component above the threshold energy of the ^{115}In(n, n′) reactions (see Fig. 4) and this compensates for the intensity difference seen in Fig. 3 resulting in a more or less symmetric distribution relative to the central value at $z = 0$.

The calculated-to-experimental value (C/E) for the high threshold reaction, ^{90}Zr(n, 2n)^{89}Zr, [E_{th} ~ 12 MeV] is shown in Fig. 6 where the values are within 2–5% (MCNP, DOT3.5) and ~ −10% (DOT5.1). The C/E values for the ^{115}In(n, n′) reaction are shown in Fig. 7. The values obtained by JAERI (DOT3.5) are less than 5% as compared to measurements while they are within −18% to +10% in the U.S. calculations with the largest deviations occuring at the front and back ends. It was noticed for other low-threshold reactions that the C/E curves exhibit an ascending trend as one moves toward the front end ($z = 100$ cm). This could be due to discrepancies in the calculated incident spectrum. It seems that spectrum of the backward neutrons is harder than it should be in the US calculations which gives rise to lower C/E values (below unity) at locations near the backend (target side) where neutrons seen at the detector locations are mostly backward. On the other hand, at locations near the front end, the larger C/E values (larger than unity) could be due to softer spectrum for

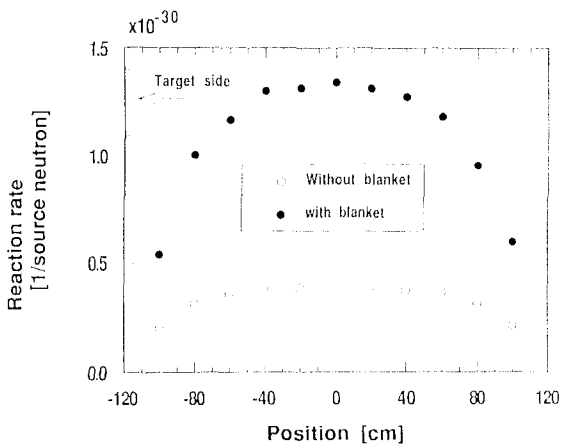

Fig. 8. Effect of the inclusion of the assembly on the axial distribution of the ^{115}In(n, n′)^{115m}In reaction (JAERI's measurements).

the forward neutrons than it should be in the US calculated incident neutron source. This combined effect results in the ascending trends seen in Fig. 7 and for other low-threshold reactions (e.g. ^{58}Ni(n, p)).

The presence of the assembly around the simulated line source results in an appreciable fraction of low-energy neutrons inside the cavity resulting from neutrons that are reflected by the assembly materials. Figure 8 shows the reaction rate distribution in the axial directions for the ^{115}In(n, n′) reaction at the inner surface of the cavity for the cases with and without the annular assembly. More than a factor of 3 increase in this reaction resulted from the inclusion of the assembly near $z = 0$ locations. Figure 9 shows the corresponding C/E values for the ^{27}Al(n, α)^{24}Na reactions with the assembly in place. At most locations, the errors are overlapping. (Note: Errors in the Monte Carlo calculations include both the statistical calculational errors and the experimental errors. Errors in the DOT calculations are only the experimental errors.) The ascending trends in the C/E values obtained by the US that are observed for the low-threshold reactions still persist but with a lesser extend, especially for these reactions that have relatively high threshold energies (e.g. ^{27}Al(n, α)). It has also been observed that the C/E values obtained by the DOT3.5 calculations (JAERI) are always larger than those obtained by the MORSE-DD code by 10–15% for low energy response reactions and by ~ 5–10% for some (n, p) reactions that have relatively large threshold energies [e.g. ^{56}Fe(n, p)^{56m}Fe, E_{th} ~ 5 MeV].

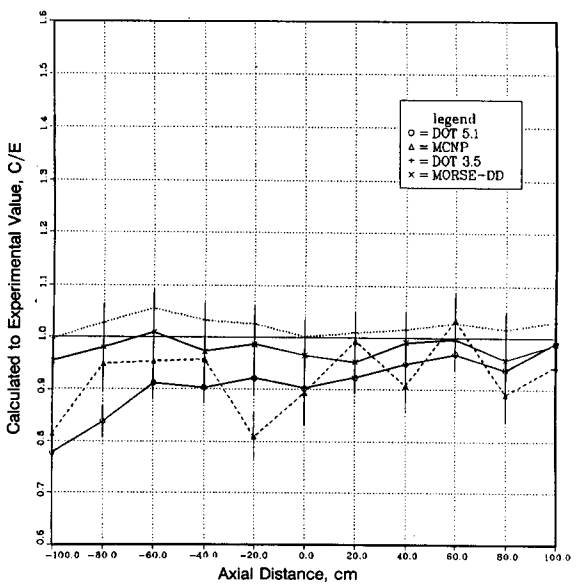

Fig. 9. C/E Values for the ^{27}Al(n, α)^{24}Na reactions in the axial direction (with assembly).

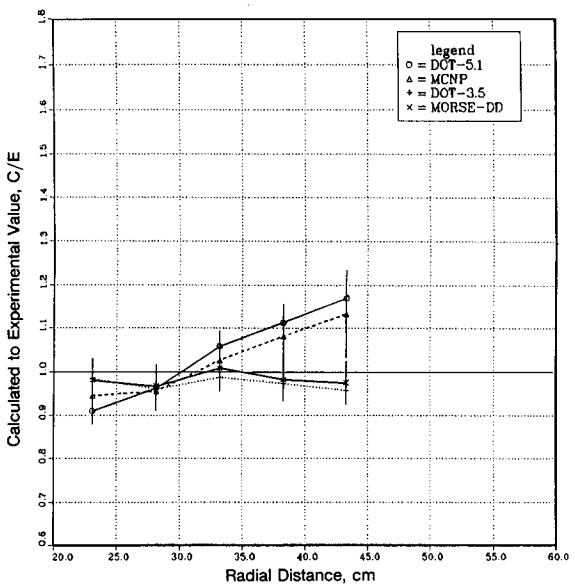

Fig. 10. C/E values for the ^{90}Zr(n, 2n)^{89}Zr reaction in the radial direction along drawer B.

In general, the agreement between the JAERI's calculations for the several reaction rates considered without the assembly is within 5% while it is within 10% when the assembly is in place. Those obtained by the US are within 10% (without the assembly) and within 10–20% (with the assembly).

4.2. In-system reaction rates

Several multifoil activation rates were measured along the axes of drawer B and C. Figure 10 shows the C/E value along the axis of drawer B for the ^{90}Zr(n, 2n)^{89}Zr reactions. The C/E values tend to increase in the US calculations and become greater than unity than those obtained by JAERI as one moves deeper inside the assembly. In this context, fig. 11 shows the C/E values for the integrated spectrum above 10 MeV as function of depth inside drawer B. The values shown are generally below unity but they are insensitive to depth. This observation and the ascending trend in the C/E values for ^{90}Zr (n, 2n) reactions (both in DOT5.1 and MCNP calculations) suggest that the energy-dependent cross-section for this reaction requires correction in the U.S. calculations as the reaction rate is the integral of the spectrum and the cross-section over the energy range above its threshold energy. The

needed correction is understandable as the measured cross-section is susceptible to large uncertainties particularly near the threshold energy due to its rapid rise. Additionally, the multigroup cross-section used in DOT5.1 calculations (30-g) will induce errors in the ^{90}Zr(n, 2n) reaction rate as a function of depth due to the limitations of the fewer energy groups at and above the threshold energy for this reaction as it is also the case for the ^{58}Ni(n, 2n) reaction (not shown). Note from Fig. 10 that the C/E values obtained by the MORSE-DD code are larger than those obtained by DOT3.5 (JAERI). This indicates that in the MORSE-DD calculations, more of high energy neutrons are transmitted deep inside the assembly than those obtained by the DOT3.5 calculations. Consequently, the low energy neutrons at the surface of the cavity and at locations nearby the first wall are more than those predicted by the MORSE-DD code. This leads to larger C/E values for low energy threshold reactions such as ^{115}In(n, n')^{115m}In at these front locations. This can be seen in the C/E curve for that reaction shown in Fig. 12 along the center axis of drawer B. Thus, in the DOT3.5 calculations, the reflected component of neutrons that reach the inner cavity is larger than the one predicted by the MORSE-DD code. This could explain the larger C/E values obtained by DOT3.5 code along the axis ($z = -100$ cm to $z = 100$ cm) at the face of the inner cavity shown in Fig. 9. The features of the C/E curves for other reactions are as follows: ^{27}Al(n, α) is within

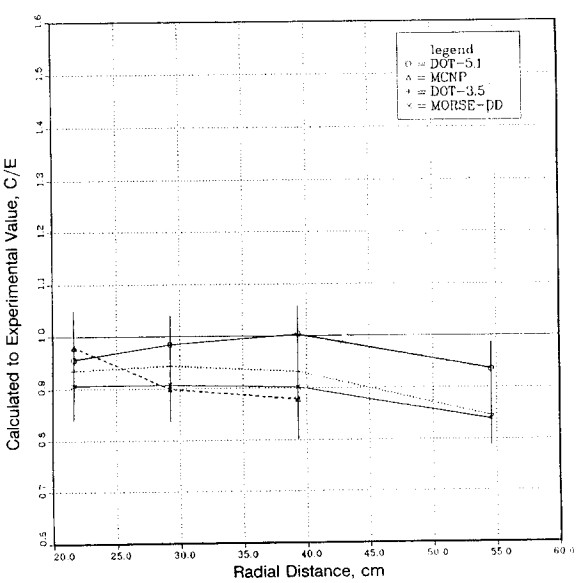

Fig. 11. Integrated neutron spectrum, $E > 10$ MeV, along the axis of drawer B.

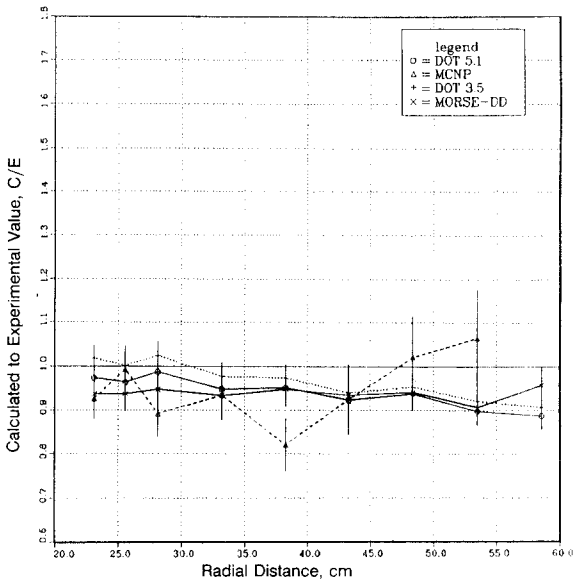

Fig. 12. C/E values for the ^{115}In(n, 2n)^{115m}In reaction in the radial direction along drawer B.

5% (JAERI) and 10% (US); ^{58}Ni(n, p) is within 2–10% (JAERI) and 2–15% (US); ^{93}Nb(n, 2n) is less than 5% (JAERI) and 2–10% (US), and for the ^{58}Ni(n, 2n) reactions, the agreement is within 5% (JAERI) with a tendency to worsen toward the back locations. As was indicated previously [11], the cross-section for this reaction should be increased by 20–25% in ENDF/B-V since at most locations, the C/E values obtained by the US are lower than unity. As for the ^{197}Au(n, γ) reactions it was observed in all the calculations that the C/E values are always less than unity by as much as 35%, particularity at locations towards the open ends of the assembly. The room-returned neutrons need thus to be further examined.

4.3 Tritium production rate

Figure 13 shows the C/E value for T_7 using the NE2 13 indirect method for measurements inside drawer B. The agreement with measurements is within $\pm 5\%$ (US) and within -10% in JAERI's calculations. In drawer C, the agreement is within $\pm 10\%$ (US) and is within $\pm 5\%$ (JAERI). It could be said that the prediction accuracy for T_7 is generally within + 10% with the NE213 method and within $\pm 15\%$ with the Li_2O pellet detectors (not shown).

The C/E values for T_6 with the Li glass detectors show an agreement within 10–15% except near the first

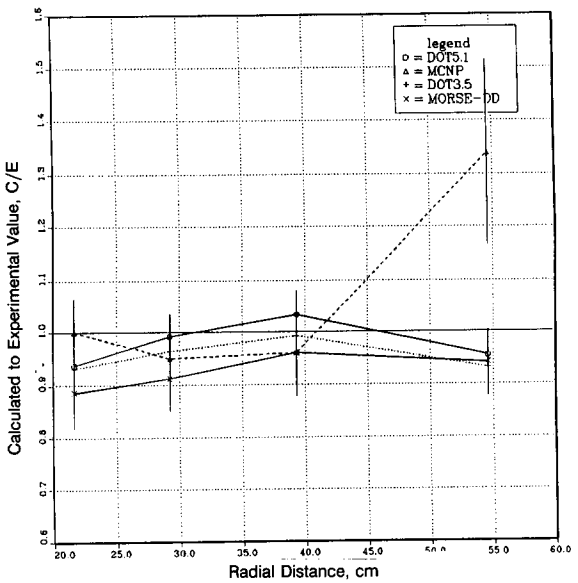

Fig. 13. C/E values of tritium production rate from $^{7}Li(T_7)$ in the radial direction along drawer B (NE213 Measurements).

wall where the agreement is within 20–30%. However, with the Li_2O pellet detectors, the agreement is better. It is within 10% (JAERI) and ±10% (US) as can be seen from Fig. 14.

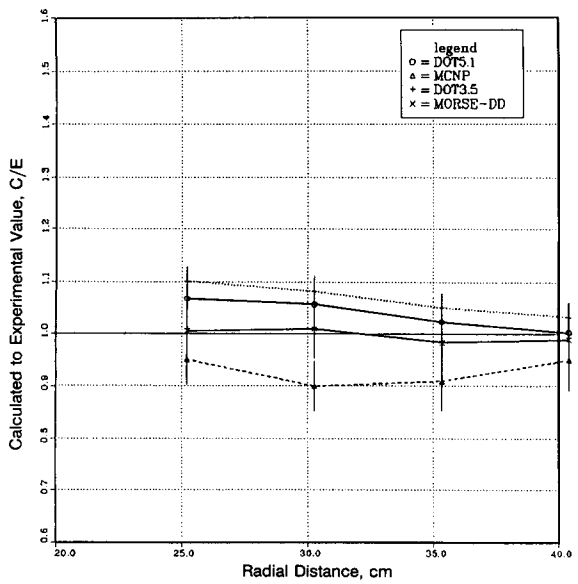

Fig. 14. C/E values for tritium production rate from $^{6}Li(T_6)$ in the radial direction along drawer B (Li_2O pellet measurements).

5. Summary

In Phase IIIA, integral fusion neutronics experiment with a line source has been performed to better simulate the incident neutron source conditions found in Tokamak reactors. A simulated line source was generated whose characteristics have been examined by various flux and foil activation measurements (with and without the annular test assembly in place) and comparison was made to calculations with various codes and nuclear data. The agreement with foil activation measurements is within 5–10% (bare line source) and within 10–20% (with the annular assembly surrounding the line source). Measurements inside the assembly indicated good agreement within 5% for some reaction rates and within 10% for some others. Tritium production rate from ^{7}Li (T_7) is generally predicted within 10–15% while the prediction accuracy for tritium production from ^{6}Li (T_6) is within 10–20%. Tritium production rate from natural Li is well predicted (5–10%).

Preparation for future experiments utilizing the simulated line source is in progress. In phase IIIA experiment, emphasis was placed on the impact of shifting from point source experiments to line source experiments on the blanket characteristics and the associated uncertainties in their predictions. One candidate experiment in the future is to study the impact of axial heterogeneities and/or poloidal asymmetry effects on these characteristics [13,14]. On-going activities are in progress to define the next experiment planned for October–November, 1991 experimental period within the USDOE/JAERI collaborative Program on Fusion Neutronics.

References

[1] T. Nakamura and M.A. Abdou, Summary of Recent Results from the JAERI/US Fusion Neutronics Phase I Experiment, Fusion Technol. 10 (1986) 541–547.

[2] M.Z. Youssef, C. Gung, M. Nakagawa, T. Mori, K. Kosako and T. Nakamura, Analysis and Intercomparison for Phase I Fusion Integral Experiments at the FNS Facility, Fusion Technol. 10 (1986) 549–563.

[3] Z. Youssef, M.A. Abdou, C. Gung, R.J. Santoro, R.G. Alsmiller, J.M. Barnes, T.A. Gabriel, M. Nakagawa, T. Mori, K. Kosako, Y. Ikeda and T. Nakamura, Phase I Fusion Integral Experiments, Vol. II: Analysis, UCLA-ENG-88-15, University of California, Los Angeles (September 1988). See also JAERI-M-88-177, Japan Atomic Energy Research Institute (August 1988).

[4] M. Nakagawa, T. Mori, K. Kosako, T. Nakamura, M.Z. Youssef, Y. Watanabe, C.Y. Gung, R.T. Santoro, R.G.

Alsmiller, J. Barnes and T.A. Gabriel, Analysis of Neutronics Parameters Measured in Phase II Experiments of JAERI/US Collaborative Program on Breeder Neutronics, Part I: Source Characteristics and Reaction Rate Distribution, Fusion Engr. and Design 9 (1989) 315–322.

[5] Y. Oyama, K. Tsuda, S. Yamaguchi, Y. Ikeda, C. Konno, H. Maekawa and T. Nakamura, Phase II Experimental Results of JAERI/USDOE Collaborative Program on Fusion Blanket Neutronics Experiments, Fusion Engr. and Design 9 (1989) 309–313.

[6] M.Z. Youssef, Y. Watanabe, C.Y. Gung, M. Nakagawa, T. Mori and K. Kosako,, Analysis of Neutronics Parameters Measured in Phase II Experiments of the JAERI/US Collaborative Program on Fusion Blanket Neutronics, Part II: Tritium Production and In-System Spectrum, Fusion Engr. and Design 9 (1989) 323–332.

[7] Y. Oyama, S. Yamaguchi, K. Tsuda, Y. Ikeda, C. Konno, H. Maekawa, T. Nakamura, K.G. Porges, E.F. Bennet and R.F. Mattas, Phase IIB Experiments of JAERI/USDOE Collaborative Program on Fusion Blanket Neutronics, Fusion Technol. 15 (2) Part 2B (1989) 1293–1298.

[8] M.Z. Youssef, Y. Watanabe, M.A. Abdou, M. Nakagawa, T. Mori, K. Kosako and T. Nakamura, Comparative Analysis for Phase IIA and IIB Experiments of the US/JAERI Collaborative Program on Fusion Breeder Neutronics, Fusion Technol. 15 (2) Part 2B (1989) 1299–1308.

[9] Y. Ikeda, C. Konno, Y. Oyama, K. Oishi, and T. Nakamura, Determination of Neutron Spectrum in D–T Fusion Field by Foil Activation Technique, Fusion Technol. 15 (2) Part 2B(1989) 1287–1292.

[10] M.Z. Youssef, M.A. Abdou, Y. Watanabe and P.M. Song, The US/JAERI Collaborative Program on Fusion Neutronics; Phase IIA and IIB Fusion Integral Experiments, The US Analysis, UCLA-ENG-90-14, University of California at Los Angeles (December 1989).

[11] M. Nakagawa, T. Mori, K. Kosako, Y. Oyama and T. Nakamura, JAERI/US Collaborative Program on Fusion Blanket Neutronics, Analysis of Phase IIA and IIB Experiments, JAERI-M-89- 154, Japan Atomic Energy Research Institute (October 1989).

[12] M.S. Youssef, A. Kumar, M. Abdou, M. Nakagawa, K. Kosako, Y. Oyama and T. Nakamura, Analysis for Heterogeneous Blankets and Comparison to Measurements: Phase IIC Experiments of the USDOE/JAERI Collaborative Program on Fusion Neutronics, Fusion Technol. 19 (3) (1991) 1891–1899.

[13] M.Z. Youssef, Y. Watanabe, A. Kumar, Y. Oyama and K. Kosako, Analysis for the Simulation of a line source by A 14 MeV moving point source and impact on blanket characteristics: The USDOE/JAERI Collaborative Program on Fusion Neutronics, ibid (1991) 1843–1852.

[14] T. Nakamura, Y. Oyama, Y. Ikeda, C. Konno, H. Maekawa, K. Kosako, M. Youssef and M. Abdou, A line D–T Neutron Source Facility for Annular Blanket Experiment: Phase III of the JAERI/USDOE Collaborative Program on Fusion Neutronics, ibid (1991) 1873–1878.

[15] Y. Oyama, C. Konno, Y. Ikeda, H. Maekawa, K. Kosako, T. Nakamura, A. Kumar, M. Youssef, M. Abdou and E. Bennet, Annular Blanket Experiment Using A Line DT Neutron Source: Phase IIIA of the JAERI/USDOE Collaborative Program on Fusion Neutronics, ibid (1991) 1879–1884.

[16] C. Konno, Y. Oyama, Y. Ikeda, K. Kosako, H. Maekawa, T. Nakamura, A. Kumar, M. Youssef and M. Abdou, Measurements of the Source Term for Annular Blanket Experiment with A Line Source: Phase IIIA of the JAERI/USDOE Collaborative Program on Fusion Neutronics, ibid (1991) 1885–1890.

[17] Y. Oyama, C. Konno, Y. Ikeda, H. Maekawa, K. Kosako, T. Nakamura, A. Kumar, M.Z. Youssef and M.A. Abdou, Phase-III Experimental Results of JAERI/USDOE Collaborative Program on Fusion Neutronics," this issue, (1991).

[18] W.A. Rhoades and R.L. Childs, An Updated Version of the DOT4 (version 4.3) One-and-Two-Dimensional Neutron/Photon Transport Code, ORNL-5851, Oak Ridge National Laboratory, (April, 1982). Also, see CCC-429, Radiation Shielding Information Center, RSIC (1982).

[19] L.P. Ku and J. Kolibal, RUFF-A Ray Tracing Program to Generate Uncollided Flux and First Collision Source Moments for DOT4, A User's Manual, EAD-R-16, Plasma Physics Laboratory, Princeton University (1980).

[20] R.A. MacFarlane, TRANSX-CTR: A Code for Interfacing MATXS Cross-Section Libraries to Nuclear Transport Codes for Fusion Systems Analysis, LA-9863-MS, Los Alamos National Laboratory (February 1984).

[21] DOT3.5: Two-Dimensional Discrete Ordinates Radiation Transport Code, CCC-276, Radiation Shielding Information Center, RSIC, Also, see W.A. Rhoades and F.R. Mynett, The DOT III Two-Dimensional Discrete Ordinates Transport Code, ORNL-TM-4280, Oak Ridge National Laboratory (September 1973).

[22] M. Nakagawa and T. Mori, MORSE--DD, A Monte Carol Code Using Multigroup Double Differential Form Cross-sections, JAERI-M84-126, Japan Atomic Energy Research Institute (July 1984).